DYNAMIC BUCKLING OF THIN-WALLED BEAM-COLUMNS WITH CHANNEL CROSS-SECTION SUBJECTED TO BENDING

M. URBANIAK, T. KUBIAK
Department of Strength of Materials, Lodz University of Technology,
Stefanowskiego 1/15, 90-924 Łódź, Poland

This paper deals with dynamic buckling of thin-walled beam-columns with channel cross-section subjected to pure bending. Different length of beams was taken into account. Assumed boundary conditions correspond to a simple support. The problem was solved by finite element method and analytical-numerical method. In order to determine the critical load pulse amplitudes there were used criteria defined by Volmir and Budiansky-Hutchinson. The results obtained from both methods were compared.

1. INTRODUCTION

Thin-walled structures are commonly used as components for cars, boats, aeroplanes, cranes and warehouses. The stability loss of thin-walled structures subjected to static load is a very well-known phenomenon and its investigations have been discussed extensively in the world literature. First studies on dynamic buckling can be found in publications performed by Volmir [18] and Budiansky [2], [6]. Volmir [18] Weller, Abramovich and Yaffe'a [19], Abramovich and Grunwald [2], Ari-Gur and Simonetta [3] in their works investigated dynamic response of thin plates. The dynamic buckling phenomenon of thin plates and thin-walled columns with plated walls can be found in [12] and [13]. The dynamic response is described by strengthening the amplitude of initial geometrical imperfection. Response of thin-walled structures to pulse loading depends on the type of structure (rod, plate, shell), the value of the load amplitude, pulse shape and its duration. For a pulse with a very short duration and high load amplitude we are dealing with the impact phenomenon. In the case of the pulse of low load amplitude and a very long duration time the problem becomes quasi-static. When the pulse load amplitude is comparable with the static critical load and the pulse duration corresponds to the period of natural vibration frequencies, it can be said the dynamic buckling problem occurs. In the dynamic buckling analysis the effects of dumping are often neglected [11]. It is well known that equilibrium path for plates with initial geometrical imperfection have no bifurcation points, so the critical buckling dynamic characteristic quantity cannot be clearly defined. Therefore, it is necessary to define the criteria [16] allowing to designate critical amplitude of the pulse load. Author decided to use three criteria due to the easiest way of their application.

Volmir [18] was one of the first scientists who had analysed buckling of thin plates subjected to pulse loading. His criterion state that:

Dynamic critical load corresponds to the amplitude of pulse load (of constant duration) at which the maximum plate deflection is equal to some constant value k (k - half or one plate thickness).

Budiansky and Hutchinson[5], [6], [8] formulated criterion for shell structures but also it can be used for plate structures [4], [14], [15], [17] and stated that:

Dynamic stability loss occurs when the maximum deflection grows rapidly with the small variation of the load amplitude.

The applied analytical-numerical method is based on the asymptotic Koiter's theory for conservative systems for the second-order approximation. In order to obtain equations of motion, the non-linear theory of orthotropic thin-walled plates has been modified in such a way that additionally it accounts for all components of inertia forces.

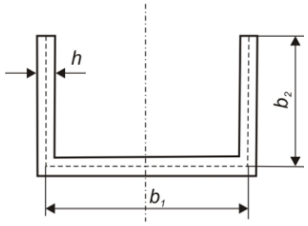

Fig. 1. Cross-section of the beam under analysis

2. FORMULATION OF THE PROBLEM

The numerical calculations were performed for exemplary thin-walled girder with C-shape cross-section (Fig.1) with the following dimensions: b_1 = 50mm, b_2 = 25mm, h = 0.5mm, and different length of the column L (39mm, 78mm, 117mm, 156mm). The assumed above lengths L are corresponded to the case with the minimal buckling load for number of half waves m equal 1, 2, 3 and 4. The material properties were assumed to be the same as for steel: $E = 2 \cdot 10^5$MPa, $\upsilon = 0.3$. The problem was solved in the elastic range. Rectangular pulse shape was taken into consideration because this shape is most dangerous [21]. Similarly to the other works that deal with dynamic buckling the dynamic load factor *DLF* defined as the ratio of the pulse amplitude to the static buckling load was introduced.

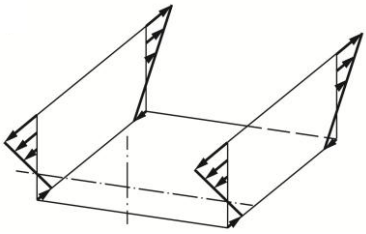

Fig. 2. Loading scheme

The scheme of load is presented in Fig. 2, considered loading is bending. It was assumed that the bending occurs round an axis, for which the second moment of area is smallest. Therefore, the FEM model is prepared in such a way that on the neutral axis of bending in the ending sections there were nodes, for which the displacement in the x

direction was set to zero (Fig. 3). Boundary condition of the loaded edges is provided by requiring the uniform displacements in the direction normal to the wall of the girder, of all nodes located on the edge of the girder (Fig. 3). To ensure that deformations are compatible with the deflection in bending the edges normal to the neutral axis remained straight in the plane containing the wall of the column. Additionally, for all nodes located on these edges the constant rotation around the axis parallel to the neutral axis was assumed.

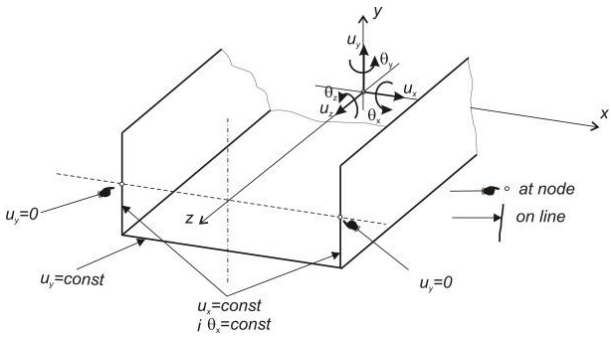

Fig. 3. Boundary conditions

2. SOLUTION METHOD

The problem was solved by analytical-numerical method (ANM) and the Finite Element Method (FEM) for comparison. ANSYS software [1] based on the Finite Element Method was used to conduct numerical calculations allowing to find dynamic response of girder segments subjected to pulse loading. The pulse duration T_p was set based on period of natural vibration. The critical load – in this case the critical bending moment (M_{bcr}) was used to determine the dynamic load factor *DLF*. The buckling or modal mode was used to set the initial imperfection with the amplitude corresponding to the thickness of the considered girder wall. The dimensionless amplitude of initial imperfection was assumed as $\xi^* = 0.01\ w_{max}/h$ (where w_{max} is the maximal normal to the wall displacement and h is the girder wall thickness). The results of these calculations were used as input to the analysis of the dynamic behaviour of the structure in time, during and immediately after exposure of pulsed load. In the analysis of the dynamic response the equilibrium equation is supplemented by the dynamic blocks, and takes the form:

$$\{\mathrm{P}\} = [\mathrm{M}]\cdot\{\ddot{\mathrm{u}}\} + [\mathrm{C}]\cdot\{\dot{\mathrm{u}}\} + [\mathrm{K}]\cdot\{\mathrm{u}\}, \tag{1}$$

where {P} is the vector of nodal forces, [M] is the mass matrix, [C] is a damping matrix and {u} is the vector of nodal displacements.

As it has been shown in many studies (for example [7]) for the short-term load the damping effect can be neglected what leads to the simplification of equation (1) to the form:

$$\{P\} = [M] \cdot \{\ddot{u}\} + [K] \cdot \{u\} \quad . \tag{2}$$

After replacing the time derivatives of displacements {ü} by differences displacement {u} in successive discrete moments of time t, the new static equilibrium equation taking into account the inertia forces [M] {ü} is obtained for the each time step and therefore it is possible to apply the algorithms used in the analysis of static. Time integration in the *ANSYS* program is done using the Newmark method and solution of equations in successive time steps is made by Newton-Raphson algorithm.

This approach allows analysing the behaviour of the structure subjected to pulse loading. Discretisation of thin-walled girders was performed with the quadrilateral; four nodes shell elements (Fig. 4) with six degrees of freedom (three orthogonal displacements and three rotations around the axis in the plane of the element) at each node.

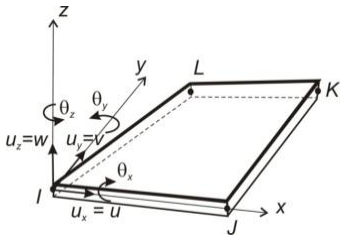

Fig. 4. Shell element [1]

The analytical-numerical method [10], [14] which allows one to analyse the static buckling, postbuckling behaviour and dynamic responses of thin-walled structures composed of plates, made of isotropic or orthotropic materials was employed. The problem was solved in the elastic range. It is assumed that the loaded edges remain straight and parallel during loading. Additionally, it is assumed that normal and shear forces disappear along the not loaded edges.

For each plate (*i*-th girder wall) geometrical relationships (3) are assumed in order to enable the consideration of both out-of-plane and in-plane bending:

$$\begin{aligned} \varepsilon_{ix} &= u_{i,x} + \tfrac{1}{2}(w_{i,x}^2 + u_{i,x}^2 + v_{i,x}^2) \\ \varepsilon_{iy} &= v_{i,y} + \tfrac{1}{2}(w_{i,y}^2 + u_{i,y}^2 + v_{i,y}^2) \\ 2\varepsilon_{ixy} &= \gamma_{ixy} = u_{i,y} + v_{i,x} + w_{i,x}w_{i,y} + u_{i,x}u_{i,y} + v_{i,x}v_{i,y} \end{aligned} \tag{3}$$

where: u_i, v_i, w_i - displacement components of the middle surface of the *i*-th wall (Fig. **5**) in the x_i, y_i, and z_i directions, respectively.

The Hamilton's Principle, taking into account Lagrange's description, full Green's strain tensor for thin plates and Kirchhoff's stress tensor, were employed to obtain the differential equations of motion (4).

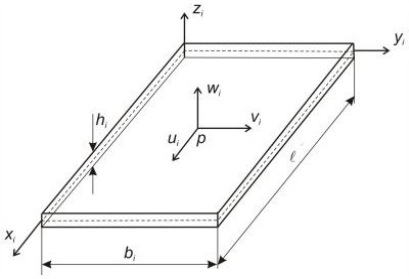

Fig. 5. Plate model for each girder wall [12]

$$
\begin{aligned}
&-\rho_i h_i \ddot{u}_i + N_{xi,x} + N_{xyi,y} + \left(N_{yi}u_{i,y}\right)_{,y} + \left(N_{xi}u_{i,x}\right)_{,x} + \left(N_{xyi}u_{i,x}\right)_{,y} + \left(N_{xyi}u_{i,y}\right)_{,x} = 0 \\
&-\rho_i h_i \ddot{v}_i + N_{xyi,x} + N_{yi,y} + \left(N_{xi}v_{i,x}\right)_{,x} + \left(N_{yi}v_{i,y}\right)_{,y} + \left(N_{xyi}v_{i,x}\right)_{,y} + \left(N_{xyi}v_{i,y}\right)_{,x} = 0 \\
&-\rho_i h_i \ddot{w}_i + \left(N_{xi,x} + N_{xyi,y}\right)w_{i,x} + \left(N_{yi,y} + N_{xyi,x}\right)w_{i,y} + N_{xi}w_{i,xx} + N_{yi}w_{i,yy} + \\
&+ 2N_{xyi}w_{i,xy} + M_{xi,xx} + 2M_{xyi,xy} + M_{yi,yy} = 0
\end{aligned}
\tag{4}
$$

The expansion of the dynamic displacement field [9] has been assumed as follows:

$$U \equiv (u, v, w) = \lambda U_i^{(0)} + \xi U_i^{(1)} + \xi^2 U_i^{(2)}, \tag{5}$$

where: λ is a load factor; $\xi = w/h_1$ is a mode amplitude (normalized, in the given case, by the condition of equality of the maximal deflection to the thickness of the first component plate h_1); $U_i^{(0)}$ is a displacement field for the prebuckling state; $U_i^{(1)}$ are linear buckling modes; $U_i^{(2)}$ are second-order displacement fields.

The static part (inertia forces have been neglected) of the system of ordinary differential equilibrium equations (4), the first and second order approximations in the *xy* plane (Fig. 5) have been solved with a modified transition matrix method. The state vector at the final edge based on the state vector at the initial edge has been found by a numerical integration of differential equations (4) along the transverse direction, using the Runge-Kutta formulae by means of the Godunov orthogonalization method [10], [14], [20]. The above-mentioned method allows for finding the nonlinear postbuckling coefficients: a_0, a_1, a_{111}, a_{1111} applied in the equation describing the postbuckling equilibrium path [10].

In the dynamic analysis (while finding the frequency of natural vibration [20]), the independent non-dimensional displacement ξ and the load factor λ become a function dependent on time. Then, Lagrange's equations are as follows:

$$\frac{1}{\omega_0^2}\xi_{,tt} + \left(1 - \frac{\lambda}{\lambda_{\min}}\right)\xi + b_{111}\xi^2 + b_{1111}\xi^3 + \ldots = \xi^* \frac{\lambda}{\lambda_{\min}}, \tag{6}$$

where: $\lambda_{\min}$ is the critical load factor corresponding to the first buckling mode (minimal buckling load), and:

$$\omega_0^2 = \frac{a_1}{m}, \quad b_{111} = \frac{a_{111}}{a_1}, \quad b_{1111} = \frac{a_{1111}}{a_1}, \quad T_p = \frac{2\pi}{\omega_0}. \tag{7}$$

The initial conditions are of the form:

$$\xi(t=0) = 0; \quad \frac{\partial \xi}{\partial t}(t=0) = 0. \tag{8}$$

The equations of motion (6) are solved with the numerical Runge-Kutta method.

3. RESULTS OF CALCULATIONS

Assumed lengths of the analyzed beams were obtained from stability analysis (eigenvalue method) as length where critical value of bending moment were minimum (Fig. 6). Following critical lengths (L_{cr}) correspond to increasing number of half-waves (m) on web of the beam. Values of length and correspond to them pulse duration and bending moment are presented in Table 1. Critical values of bending moment obtained from both methods are similar, differences between values are about 4%.

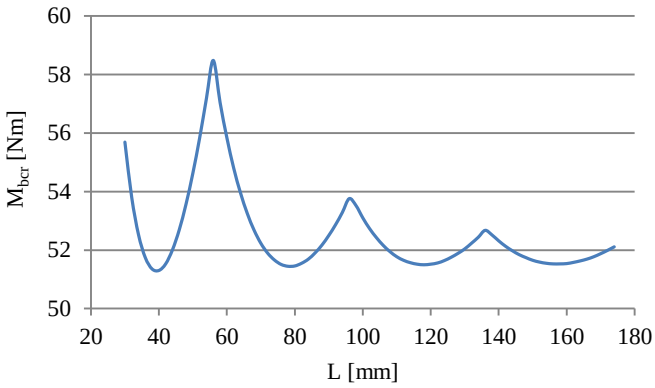

Fig. 6. Critical value of bending moment (M_{bcr}) versus length of the beam

The dynamic buckling of thin-walled channel cross-section girders was analysed based on dimensionless deflection ($\xi = w/h$, where w – deflection) as a function of dynamic load factor. The deflection w was measured in the same point in all cases – on the middle of the length and in the middle of the width of the beams web and on node placed on the middle of first half-wave of buckling mode.

The results of numerical calculations are presented on Fig. 7 when displacements were measured on the middle of the web of the beam. It can be noted that with increasing length of the beam, the curve of dynamic response of structure are flattening. Straight line representing nondimensional displacement vs. dynamic load factor (Fig. 7) means that dynamic response of the structure is not corresponding the local, global or even coupled buckling but it is linearly change of the maximal deflections for applied amplitude of

pulse loading (the structure is bended). In that the critical value of load case cannot be determined from well know criteria (except of Volmir criterion).

Table 1. Lengths of the analyzed beams and critical values of bending moment and pulse duration corresponding to them

	m=1	m=2	m=3	m=4
L_{cr} [mm]	39	78	117	156
M_{bcr} [Nm] (FEM)	51.28	51.45	51.50	51.53
M_{bcr} [Nm] (AN)	53,66	53,66	53,66	53,66
T_p [ms]	0.86	1.89	2.55	2.94

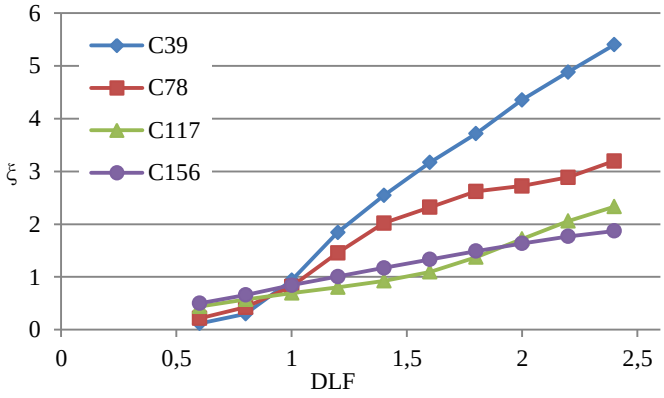

Fig. 7. Dimensionless displacement vs. dynamic load factor curves for different lengths of beam (displacement measured on middle of the web)

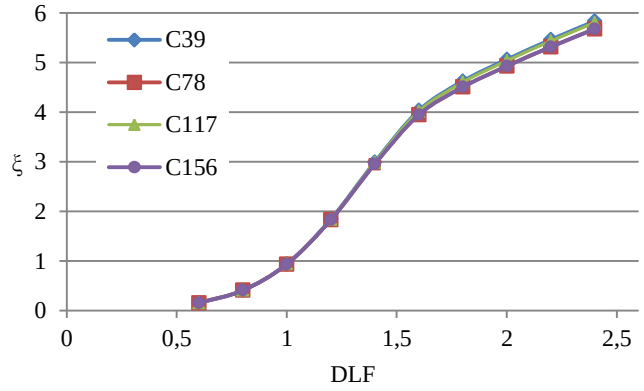

Fig. 8. Dimensionless displacement vs. dynamic load factor curves for different lengths of beam obtained from analytical-numerical method

The results of calculations obtained from *AN* method are presented in Fig. 8. It can be noted that for each lengths of beams dynamic responses are the same. These results are obtained with local buckling and corresponding number of half-waves assumption (the longitudinal edges deflections were not taken into account), what explain above statement and results presented in Fig. 8.

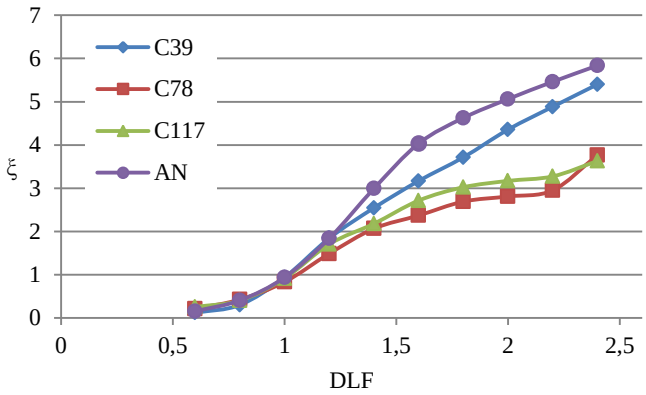

Fig. 9. Dimensionless displacement vs. dynamic load factor curves for different lengths of beam (displacement measured on node placed on the middle of first half-wave of buckling mode)

In Fig. 9 the results of calculations for case when displacement is measured on node located on the middle of first half-wave of buckling mode and results obtained from analytical-numerical method are presented. Similarity of curves obtained from both methods can be noted. Critical values of *DLF* determined from *FEM* method for every length of beams are equal and value obtained from *AN* is similar to them (Table 2).

Table 2. Critical values of *DLF* for analysed beams

	C39	C78	C117	AN
Volmir criterion	1.1	1.1	1.1	1.1
Budiansky-Hutchinson criterion	1.0-1.2	1.0-1.2	1.0-1.2	1.2-1.4

4. CONCLUSIONS

Taking into consideration presented results of calculations, it can be said that only local dynamic buckling for beams subjected to pure bending is possible to determine. Dynamic response corresponding to local buckling can be observed when displacement is measured on node placed on the middle of first half-wave of buckling mode. For long beams dynamically loaded with bending moment response of the structure is not corresponding to local, global or coupled buckling, there is no rapid grow of deflection with the small variation of load amplitude (structure is bended). Therefore none of known criteria can be used to determine critical value of load amplitude. Results obtained from

analytical-numerical method has a good agreement with results obtained from *FEM* when displacement is measured on node placed on the middle of first half-wave of buckling.

ACKNOWLEDGEMENTS

This publication is a result of the research work carried out within the project subsidized over the years 2009-2012 from the state funds designated for scientific research (MNiSW - N N501 113636).

REFERNECES

[1] ANSYS User's Guide rev. 12.1, Ansys, Inc, 2011.
[2] Abramovich H, Grunwald A. Stability of axially impacted composite plates. Composite Structure, 32, 1995, pp.151–158.
[3] Ari-Gur J., Simonetta S.R., Dynamic pulse buckling of rectangular composite plates, Composites Part B, 28B, 1997, pp. 301-308.
[4] Bisagni C., Dynamic buckling of fiber composite shells under impulsive axial compression, Thin-Walled Structures 43, 2005, 499–514.
[5] Budiansky B., Dynamic buckling of elastic structures: criteria and estimates, Report SM-7, NASA CR-66072, 1965.
[6] Budiansky B., Hutchinson J.W., Dynamic buckling of imperfection-sensitive structures, Proceedings of the Eleventh International Congress of Applied Mechanics, Goetler H. (Ed.), Munich,1966, pp. 636-651.
[7] Cui S., Hao H., Cheng H.K., Theoretical study of dynamic elastic buckling of columns subjected to intermediate velocity impact loads, Int. J. of Mechanical Science, 44, 2002, pp. 687-702.
[8] Hutchinson J.W., Budiansky B., Dynamic buckling estimates, AIAA Journal, 4(3), 1966, pp. 525-530.
[9] Koiter T., Elastic stability and post-buckling behaviour, Proceedings of the Symposium on Nonlinear Problems, Univ. of Wisconsin Press, Wisconsin, 1963, pp. 257-275.
[10] Kolakowski Z., Kowal-Michalska K. (eds.), Selected Problems of Instabilities in Composite Structures, A Series of Monographs, Technical University of Lodz, 1999.
[11] Kounadis A.N., Gantes C., Simitses G., Nonlinear dynamic buckling of multi-dof structural dissipative system under impact loading, Int. J. Impact Engineering, 19(1), 1997, pp. 63-80.
[12] Kowal-Michalska K. (ed.), Dynamic Stability of Composite Plate Structures (*in Polish* – Stateczność dynamiczna kompozytowych konstrukcji płytowych), WNT, Warszawa, 2007.
[13] Królak M., Mania R.J. (ed.), Stability of Thin-Walled Plate Structures, Technical University of Lodz, 2011.
[14] Kubiak T., Dynamic buckling of thin-walled composite plates with varying widthwise material properties, Int. J. of Solid and Structures, 45, 2005, pp. 5555 – 5567.
[15] Kubiak T., Dynamic buckling of thin-walled girders with channel cross-section, VDI-Berichte, 1899, 2005, pp. 69 – 78.

[16] Kubiak T., Criteria for dynamic buckling estimation of thin-walled structures, Thin-Walled Structures, Vol. 45 (10-11), 2007, pp. 888-892.

[17] Petry D., Fahlbusch G., Dynamic buckling of thin isotropic plates subjected to in-plane impact, Thin-Walled Structures 38, 2000, pp. 267-283.

[18] Volmir S.A., Nonlinear Dynamics of Plates and Shells, Science, Moscow, 1972.

[19] Weller T., Abramovich H., Yaffe R., Dynamic buckling of beams and plates subjected to axial impact, Computers &Structures, 37, 1989, pp. 835-851.

[20] Teter A., Kolakowski Z., Natural frequencies of thin-walled structures with central intermediate stiffeners or/and variable thickness, Thin-Walled Structures, 41, 2003, pp. 291-316.

[21] Urbaniak M., Kubiak T., Local dynamic buckling of C-shape profile subjected to bending, Mechanics and Mechanical Engineering, Vol. 15, No 1, 2011, pp. 131-144